

Theoretical Investigation of Crystal and Electronic Structure of piezoelectric $\text{AgNb}_{0.5}\text{Ta}_{0.5}\text{O}_3$

Shivani Singh

A Dissertation Submitted to
Indian Institute of Technology Hyderabad
In Partial Fulfillment of the Requirements for
The Degree of Master of Science



भारतीय प्रौद्योगिकी संस्थान हैदराबाद
Indian Institute of Technology Hyderabad

Department of Physics

April, 2015

Declaration

I declare that this written submission represents my ideas in my own words, and where others' ideas or words have been included, I have adequately cited and referenced the original sources. I also declare that I have adhered to all principles of academic honesty and integrity and have not misrepresented or fabricated or falsified any idea/data/fact/source in my submission. I understand that any violation of the above will be a cause for disciplinary action by the Institute and can also evoke penal action from the sources that have thus not been properly cited, or from whom proper permission has not been taken when needed.

Shivani Singh.

(Signature)

Shivani Singh
(Student Name)

Ph13m1013
(Roll No)

Approval Sheet

This thesis entitled 'Theoretical investigation of Crystal and Electronic Structure of piezoelectric $\text{AgNb}_{0.5}\text{Ta}_{0.5}\text{O}_3$ ' by Shivani Singh is approved for the degree of Master of Science from IIT Hyderabad.



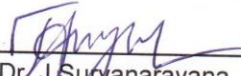
Dr. Prem Pal
Coordinator/ Examiner



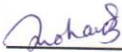
Dr. Vandana Sharma
Examiner



Dr. N. Sahu
Examiner



Dr. J. Sanyal
Examiner



Dr. J. Mohanty
Examiner



Dr. S. Hundi
Examiner



Dr. Manish K. Niranjana
Adviser



Acknowledgements

I have taken efforts in this project. However, it would not have been possible without the kind support and help of many individuals. I would like to extend my sincere thanks to all of them.

I am highly indebted to Dr. Manish Niranjana, T. Karthik and V. Sampat for their guidance and constant supervision as well as for providing necessary information regarding the project & also for their support in completing the project.

I would like to express my gratitude towards my parents & friends for their kind co-operation and encouragement which help me in completion of this project.

My thanks and appreciations also go to my colleague in developing the project and people who have willingly helped me out with their abilities.

Dedicated to

Dr. Manish Niranjana

Abstract

We present an ab-initio study of structural and electronic properties of lead-free oxide $\text{AgNb}_{0.5}\text{Ta}_{0.5}\text{O}_3$ (ANTO) in orthorhombic $Pbcm$ space group and monoclinic $p2/m$ space group. In our calculations, both the symmetries (orthorhombic $Pbcm$ and monoclinic $p2/m$) of $\text{AgNb}_{0.5}\text{Ta}_{0.5}\text{O}_3$ show small relative energy difference (~ 0.6062 eV), thus suggesting the coexistence of both the unit cells at the room temperature. Band Structure of ANTO infers that the compound is an insulator or semiconductor with direct band gap. Conduction band of ANTO, consists of Nb-4d and Ta-5d and upper level of valence band is contributed by Ag-4d and O-2p while lower level is contributed by Nb-4d and Ta-5d along with O-2p. Charge density of ANTO is uniformly spherical around Ag deducing an ionic bond between Ag-O and non uniform spherical charge density around Ta/Nb-O suggests an ionic covalent bond due to high electronegativity of O. Large phonon frequency belongs to O atom and the phonon frequency ranging in lower frequency range corresponds to Ag-O and Nb-o/Ta-O vibrations, respectively.

Content

1. Introduction	8
1.1. Oxides	8
1.2. High- κ dielectric	8
1.3. Ferroelectric Compound	9
1.4. ANTO Compound	10
2. Computational Methodology	12
2.1. DFT (density functional theory)	12
2.2. Exchange Correlation Potential	14
2.3. Ultrasoft pseudopotential	15
3. Result and Analysis of ANTO	17
3.1. Relaxed Structure	17
3.2. Density of States	20
3.3. Projected Density of States	22
3.4. Band Structure	24
3.5. Charge Density	26
3.6. Phonon	28
4. Conclusion and Discussion	32
4.1. Conclusion	32
4.2. Discussion	33
5. References	34

Chapter 1.

1. Introduction

1.1. Oxides

Oxides comprise a wide class of materials exhibiting fine crystal structures and physical properties that make them ideal candidates for a plethora of applications. Lead based piezoelectric solid solutions, such as, lead zirconium titanate (PZT) are widely used as sensors, actuators, imaging devices, accelerometers, etc. However, due to environmental concern, there is growing interest in the development of high performance lead free piezoelectrics. There has been a recent resurgence of interest in oxides in general and complex oxides in particular due to their piezoelectric, ferroelectric, ferromagnetic, ferrimagnetic, and multiferroic properties as well as, in many cases, large dielectric constants [1].

Oxide materials with large dielectric constants (so-called high- κ dielectrics) have attracted much attention due to their potential use as gate dielectrics in MOSFETs [1]. The increased interest in these materials lately stems in part from the fact they are considered to be good candidates for nonvolatile ferroelectric random- access memory (FeRAM) devices, due to their high dielectric constant values and hysteresis in their polarization vs. electric field characteristics.

1.2. High- κ Dielectrics

The term high- κ dielectric refers to a material with a high dielectric constant κ (as compared to silicon dioxide). High- κ dielectrics are used in semiconductor manufacturing processes where they are usually used to replace a silicon dioxide gate dielectric or another dielectric layer of a device [1]. Replacing the silicon dioxide gate dielectric with a high- κ material allows increased gate capacitance without the associated leakage effects. High- dielectric materials have recently become important in mainly three areas : memory cell dielectrics , passive components and gate dielectrics [1].

The gate oxide in a MOSFET can be modeled as a parallel plate capacitor. Ignoring quantum mechanical and depletion effects from the Si substrate and gate, the capacitance C of this parallel plate capacitor is given by

Where,

$$C = \frac{K\epsilon_0 A}{t}$$

A is the capacitor area

κ is the relative dielectric constant of the material

ϵ_0 is the permittivity of free space

t is the thickness of the capacitor oxide insulator

Since leakage limitation constrains further reduction of t , an alternative method to increase gate capacitance is alter κ by replacing silicon dioxide with a high- κ material.

1.3. Ferroelectric Oxide

The birth of ferroelectrics can probably be traced back to 1921 when Valashek observed nonlinear electrical properties of potassium sodium tartrate tetrahydrate, a material that was known for more than two centuries. In potassium sodium tartrate tetrahydrate compound, also known as Rochelle salt, Pierre and Jacques Curie first discovered piezoelectricity in 1880 [1]. Ferroelectrics belong to a wider class of materials called pyroelectrics, which in turn belong to a piezoelectric class. Pyroelectricity is the phenomenon that an electric charge is created in certain materials as a result of temperature change, and piezoelectricity is the ability to generate an electric potential in response to applied mechanical stress. All ferroelectric materials also exhibit piezoelectricity and pyroelectricity but not vice versa.

Ferroelectrics are a class of materials exhibiting spontaneous polarization below the ferroelectric Curie temperature (T_C), and the polarization direction can be changed by an applied electric field. At temperatures above T_C , the crystals are non-polar and no longer ferroelectric and behave like normal dielectrics. The dielectric constants of

ferroelectric materials are extremely high, especially near the Curie temperature. Ferroelectric oxides have attracted great attention for device applications, one of which is ferroelectric RAM, because of their ability to retain two stable polarization states [1]. Example of ferroelectric materials, such as BaTiO₃ (BT), Ba_xSr_{1-x}TiO₃ (BST), Pb(Zr,Ti)O₃ (PZT), SrBi₂Ta₂O₉ (SBT), AgNb_{0.5}Ta_{0.5}O₃ (ANTO).

1.4. ANTO Compound

The ANTO is a relaxor perovskite (ABO₃) with B-site being equally shared by two different cations, a property uncommon in most of the ABO₃ systems. Raman and Infrared spectroscopic techniques have been used to study various structural aspects in ANTO system and its solid solutions [2]. These techniques are advantageous as they provide precise information of local distortions and ionic configurations in the crystal structure .

Preliminary investigations have revealed that AgNb_{1-x}Ta_xO₃ solid solution, with x ≈ 0.5, as a new high- permittivity ($\epsilon_r > 400$) microwave material that is applicable in the microwave- and radio-frequency region [2].

First, studies of the structural features of a AgNb_{1-x}Ta_xO₃ solid solutions were conducted by Belayaev ^{et al}[19]. According to their findings, three different monoclinic modifications exist at room temperature in the 0 < x < 0.9 composition range. In the 0 < x < 0.4 range, there are two monoclinic distortions with a, c > b and $\beta > 90^\circ$ that change at x > 0.5 to a not equal b not equal c and $\beta > 90^\circ$ [20].

For AgTa_{0.5}Nb_{0.5}O₃ , the room- temperature phase is analogous to that of the end - member AgNbO₃ and exhibits Pbcm orthorhombic symmetry with 40 atoms per unit cell having lattice parameter $\sqrt{2}a * \sqrt{2}a * 4a$ where, a = 4 Å refers to an ideal cubic perovskite unit cell in most of the reported studies [3][4][5]. However, the crystal structure of monophasic AgTa_{0.5}Nb_{0.5}O₃ using Powder diffractometry (XRD) revealed a monoclinic unit cell of P2/m space group with 10 atoms per unit cell with cell parameter a = 3.9286 Å , b = 3.9259 Å , c = 3.9302 Å and beta angle = 90.49° [2].

In this work, we address these issues within the ab- initio density functional theoretical framework, and identify spectroscopic signature of the structure through comparison in LDA and GGA approximation of both the structures.

Chapter 2.

2. Computational Methodology

We use density functional theory (DFT) with the ultrasoft pseudopotential (USPP) method, as implemented in Plane Wave scf Package. The Generalized gradient approximations (GGA) and Local density approximation (LDA) for exchange - correlation were employed along with a standard plane wave basis set with a kinetic energy cutoff of 340 eV. The calculations are performed using the 4x4x2 Monkhorst–Pack k-point mesh for the monoclinic and orthorhombic unit cell. The calculations are converged to 10^{-6} eV/cell and the structures are relaxed until the largest force becomes less than 10^{-3} eV/Å.

2.1 Density Functional Theory (DFT)

Density functional theory is an approach for the description of ground state properties of metals, semiconductors, and insulators. The success of density functional theory (DFT) not only encompasses standard bulk materials but also complex materials such as proteins and carbon nanotubes [10][17].

The main idea of DFT is to describe an interacting system of fermions via its density and not via its many-body wave function. For N electrons in a solid, which obey the Pauli principle and repulse each other via the Coulomb potential, this means that the basic variable of the system depends only on three -- the spatial coordinates x , y , and z -- rather than $3N$ degrees of freedom [10][11].

Knowledge of the density is all that is necessary for a complete determination of all ground state properties. If one knows the exact electron density, $\rho(r)$, then this density would occur at the positions of the nuclei.

2.1.1. The Hohenberg - Kohn Theorem

The first Hohenberg-Kohn theorem asserts that the density of any system determines all ground-state properties of the system, that is, $E = E[\rho]$, where ρ is the ground-state density of the system. [11][12]

The second H-K theorem shows that there exists a variational principle for the above energy density functional $E[\rho]$. Namely, if ρ' is not the ground state density of the above system, then $E[\rho'] > E[\rho]$.

2.1.2. Consequence of H-K Theorem

Each local one-particle potential corresponds exactly to one ground state density. This permits us to express the potential as a function of the density $V[\rho]$ [11][12].

$$H|\phi_{GS}\rangle = E_{GS}|\phi_{GS}\rangle$$

where, E_{GS} is the ground state energy and $|\phi_{GS}\rangle$ is non-degenerate ground state.

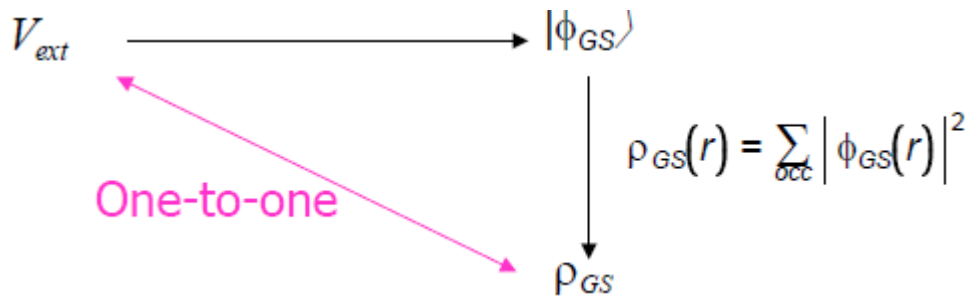


Figure 1.1 ref[11]

Ground state expectation values depend uniquely on ρ_{GS} (ground state charge density)

$$\rho_{GS} \Rightarrow V_{ext} \Rightarrow H \Rightarrow |\phi[\rho_{GS}]\rangle \Rightarrow O[\rho_{GS}] = \langle \phi[\rho_{GS}] | O | \phi[\rho_{GS}] \rangle$$

$\rho_{GS}(x,y,z)$ and not $\phi_{GS}(x_1,y_1,z_1, \dots, x_N,y_N,z_N)$ is the basic variable.

Also, Hamiltonian of H-K is same as Hartree – Fock Hamiltonian but with a term that account for electron exchange in terms of the density i.e.,

$$H = T + V_{ext} + V_{coul} + V_{xc}$$

Instead of calculating using explicit exchange DFT uses an additional function of the density V_{xc} where the x stands for exchange and the c stands for correlation. The central problem in DFT is that there is no unique prescription for how to find the exchange and correlation functionals.

2.1.3. The Kohn - Sham approach

Treat the electrons as N fictitious non-interacting particles moving in an effective potential [11][12].

$|\varphi_i\rangle \equiv$ independent particle wave function

density: $\rho_{KS} = \sum |\varphi|^2$

kinetic energy: $T_{KS} = -1/2 \sum \langle \varphi_i | \nabla^2 | \varphi_i \rangle$

The Kohn-Sham assumption is that the K-S density ρ_{KS} is equal to the true density.

Kohn-Sham energy partitioning:

$$E[\rho] = T[\rho] + E_{\text{ext}}[\rho] + E_{\text{Coul}}[\rho] + E_{\text{xc}}[\rho]$$

The Kohn-Sham equations, variational minimization of $E[\rho]$:

$$[-1/2 \nabla^2 + V_{\text{coul}}(\rho, r) + V_{\text{ext}}(\rho, r) + V_{\text{xc}}(\rho, r)] \varphi_i(r) = \varepsilon_i \varphi_i(r)$$

Local exchange-correlation functional contains all of the complexities of the many-electron system,

$$E_{\text{xc}}[\rho] = \int dr \rho(r) V_{\text{xc}}(\rho, r)$$

Solve single-particle problem instead of many-electron problem and the remaining issue is to find the appropriate exchange-correlation functional.

2.2. The Exchange - Correlation Potential

While DFT in principle gives a good description of ground state properties. The exchange-correlation potential describes the effects of the Pauli principle and the Coulomb potential beyond a pure electrostatic interaction of the electrons.

A common approximation is the local density approximation (LDA) which locally substitutes the exchange-correlation energy density of an inhomogeneous system by that of an electron gas evaluated at the local density. And other approximation is Generalized gradient approximations (GGA) are still local but also take into account the gradient of the density at the same coordinate[13][14].

2.2.1. Local Density Approximation

Local-density approximations (LDA) are a class of approximations to the exchange–correlation (XC) energy functional in density functional theory (DFT) that depend solely upon the value of the electronic density at each point in space.

In general, a local-density approximation for the exchange-correlation energy is written as [14],

$$E_{XC}^{LDA}[n] = \int \epsilon_{XC}(n)n(\vec{r})d^3r.$$

where n is the electronic density and ϵ_{xc} is the exchange-correlation energy per particle of a homogeneous electron gas of charge density n .

2.2.2. Generalized Gradient Approximation

In GGA, exchange-correlation energy is functional of electronic density as well as the gradient of electronic density [15][16][17] ,

$$E_{XC}^{GGA}[n_{\uparrow}, n_{\downarrow}] = \int \epsilon_{XC}(n_{\uparrow}, n_{\downarrow}, \vec{\nabla}n_{\uparrow}, \vec{\nabla}n_{\downarrow})n(\vec{r})d^3r.$$

GGA approximation are more accurate than LDA.

2.3. Ultrasoft - Pseudopotential

Pseudopotential is an approximate way of replacing the effect of core electron and its nucleus with effective potential for a complex system. So, Schrodinger's equation contains a modified effective potential instead of simple columbic potential. The

pseudopotential is an effective potential constructed to replace the atomic all-electron potential (full-potential) such that core states are eliminated and the valence electrons are described by pseudo-wavefunctions with significantly fewer nodes.

First-principles pseudopotentials are derived from an atomic reference state, requiring that the pseudo- and all-electron valence eigenstates have the same energies, amplitude and density outside a chosen core cut-off radius 'rc'. First-principles pseudopotentials are usually non-local, meaning that different angular momentum states feel different effective potentials, giving a potential operator of the form [21] :

$$\hat{V}_{ps} = V_{ps}^{\text{loc}} + \sum_{i,j} D_{ij} |p_i\rangle \langle p_j|$$

In Ultrasoft pseudopotential, the norm of each pseudo- wavefunction and its corresponding all-electron wavefunction are not zero identical.

Therefore mathematically [22],

$$q_{\mathbf{R},ij} = \langle \phi_{\mathbf{R},i} | \phi_{\mathbf{R},j} \rangle - \langle \tilde{\phi}_{\mathbf{R},i} | \tilde{\phi}_{\mathbf{R},j} \rangle$$

where,

$\phi_{\mathbf{R},i}$ and $\tilde{\phi}_{\mathbf{R},i}$ are the all-electron and pseudo reference states for the pseudopotential on atom of radius R.

So the normalised eigenstate of the pseudo-potential now obeys the generalized equation [22],

$$\hat{H} |\Psi_i\rangle = \epsilon_i \hat{S} |\Psi_i\rangle,$$

where,

$$\hat{S} = 1 + \sum_{\mathbf{R},i,j} |p_{\mathbf{R},i}\rangle q_{\mathbf{R},ij} \langle p_{\mathbf{R},j}|$$

For Ultrasoft pseudopotential perfect plane- wave is not required.

Chapter 3.

3. Result and Analysis of ANTO

3.1 Relaxed Structure

Theoretically obtained volume of two unit cells of $\text{AgNb}_{0.5}\text{Ta}_{0.5}\text{O}_3$ having monoclinic unit cell with $p2/m$ space group and cell parameters : $a = 7.4239775 \text{ au}$, $b = 7.4188752 \text{ au}$, $c = 7.4270 \text{ au}$ and beta angle = 90.49° (approx. 90.0°) is 818.092 au^3 having 10 atoms per unit cell [2] (from table 3.1).

Calculated, relaxed volume of $\text{AgNb}_{0.5}\text{Ta}_{0.5}\text{O}_3$ with 10 atoms in a unit cell from table 3.1 is 797.4516 au^3 with LDA potential and 813.5871 au^3 with GGA potential. The unit cell of compound AgNbO_3 and AgTaO_3 are stack in order to get the unit cell with $a=b= 7.409301 \text{ au}$ and $c= 14.820045 \text{ au}$ and approximately 0.16% error in each parameter for GGA potential. The minimum Energy obtained is -599.13784792 Ry and Fermi level is 11.2564 eV . Number of electron is 84. The Unit cell has Ag at the corner and O at the face center with Nb and Ta at the body center. Fig. 3.1 represents the monoclinic structure of unit cell of ANTO compound.

Table 3.1

Type of Unit Cell	Approximation Type	Experimental Volume	Calculated Volume	Percentage error
Monoclinic	LDA	818.092 au ³ [2]	797.451 au ³	2.5%
Monoclinic	GGA	818.092 au ³ [2]	813.5871 au ³	0.5%
Orthorhombic	LDA	3402.07au ³ [4]	3109.3739 au ³	7.83%
Orthorhombic	GGA	3402.07au ³ [4]	3219.2050 au ³	5.37%

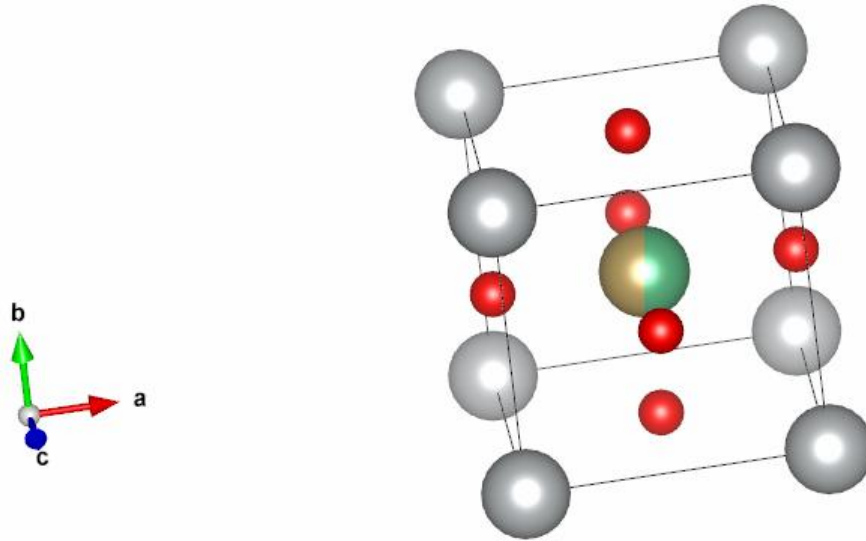


Fig.3.1. Monoclinic unit cell of $\text{Ag}(\text{NbTa})_{0.5}\text{O}_3$ with red color balls represent Oxygen, silver color balls represent Silver and Green and Golden balls are Ta and Nb respectively. Body center is shared by Nb and Ta in the unit cell.

Similarly for Orthorhombic crystal structure with Pbcm space group is analogous to that of the end-member AgNbO_3 with lattice parameters $\sqrt{2}a \times \sqrt{2}a \times 4a$ ($a \approx 4\text{\AA}$ refers to an ideal cubic perovskite cell) has unit cell volume 3402.07au^3 [4] (from table 3.1).

Relaxed volume of $\text{AgNb}_{0.5}\text{Ta}_{0.5}\text{O}_3$ with 40 atoms in a unit cell (as calculated in table 3.1) is 3109.3739au^3 with LDA potential and 3164.6754au^3 with GGA potential. The calculated lattice parameter has $a = 10.3978 \text{au}$, $b = 10.50309 \text{au}$ and $c = 29.47736 \text{au}$ and approximately 1.79% error in each parameter for GGA potential. The minimum Energy obtained is -2396.615Ry and Fermi level is 11.7614eV . Number of electron is 336. Fig. 3.2 represents the orthorhombic unit cell of ANTO compound.

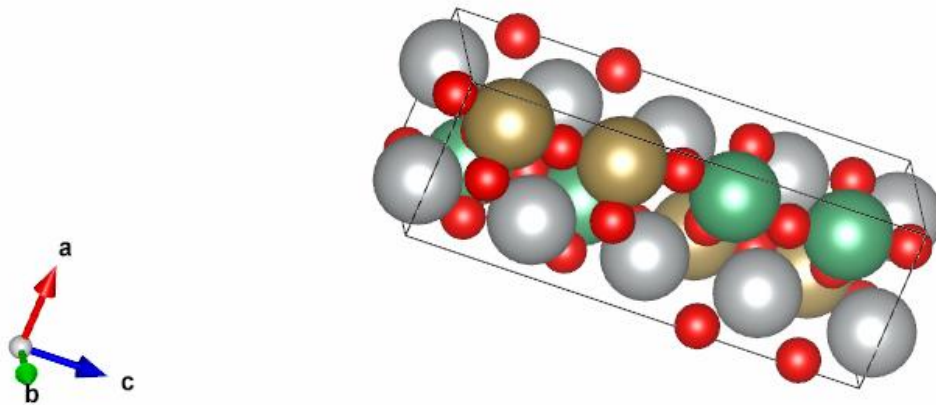


Fig. 3.2.Orthorhombic Space group with Pbcm space group with silver balls representing Silver atoms, red balls Oxygen atom, Green balls are Ta atom and Golden balls are Nb respectively.

3.2. Density of States

The Fermi level (uppermost level of valence band) of $\text{AgNb}_{0.5}\text{Ta}_{0.5}\text{O}_3$ is coming out to be 11.2564 eV after the self consistent calculation using Kohn-Sham density functional theory for monoclinic structure. The DOS curve (fig. 3.3) of $\text{AgNb}_{0.5}\text{Ta}_{0.5}\text{O}_3$ has zero electronic state at the Fermi level, indicating that $\text{AgNb}_{0.5}\text{Ta}_{0.5}\text{O}_3$ is not a metal.

The DOS can be divided into two separate regions, the valence band and the conduction band. The valence band is the collection of all occupied electronic states, while all states in the conduction band are unoccupied at $T= 0$ K. The region of energy that separates the valence and conduction bands is called band gap and it contains no electronic states at all. It is clear that applying an electric field to these materials will not lead to electron conduction as easily as it does in metals. Materials with a band gap are classified as either semiconductors if their band gap is “small” or insulators if their band gap is “wide.” The distinction between these two types of materials is somewhat arbitrary, but band gaps larger than 3 eV are typically considered wide band gaps [9][18].

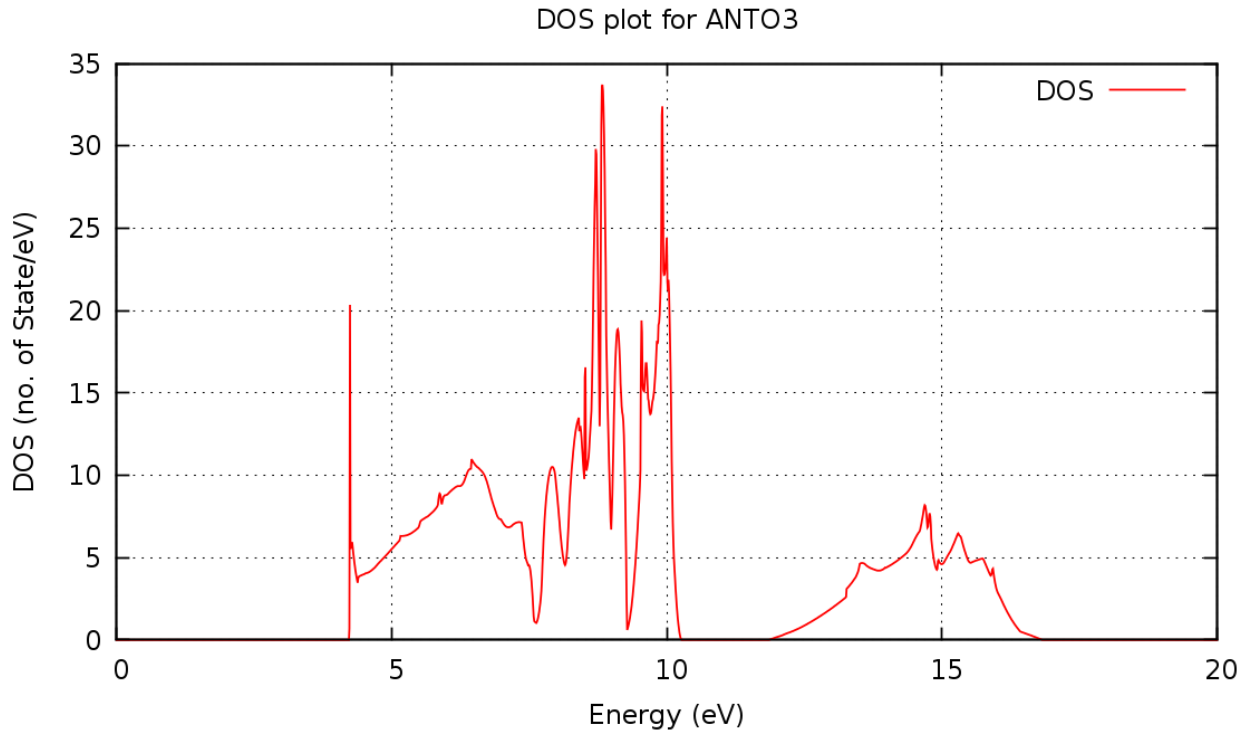


Fig 3.3. DOS plot for ANTO monoclinic structure with space group p2/m and GGA potential. Valence band ranges from approximately 4eV to 10.5 eV and Conduction band ranges from approximately 12 eV to 16 eV.

Highly available occupancy electronic state from the fig. 3.3 is in between 7 eV to 10 eV in valence band. Gap between valence and conduction band represent that the compound is an insulator or a semiconductor. A high DOS at a uppermost level of valence band energy level means that there are many states available for occupation.

Comparison between the DOS curve of orthorhombic and monoclinic structure (fig.3.4):

Fermi level for both the structure is approximately same which is between ~11.2 eV and 11.8eV. Both the plots are almost same but the occupancy state is higher in orthorhombic state than in monoclinic state.

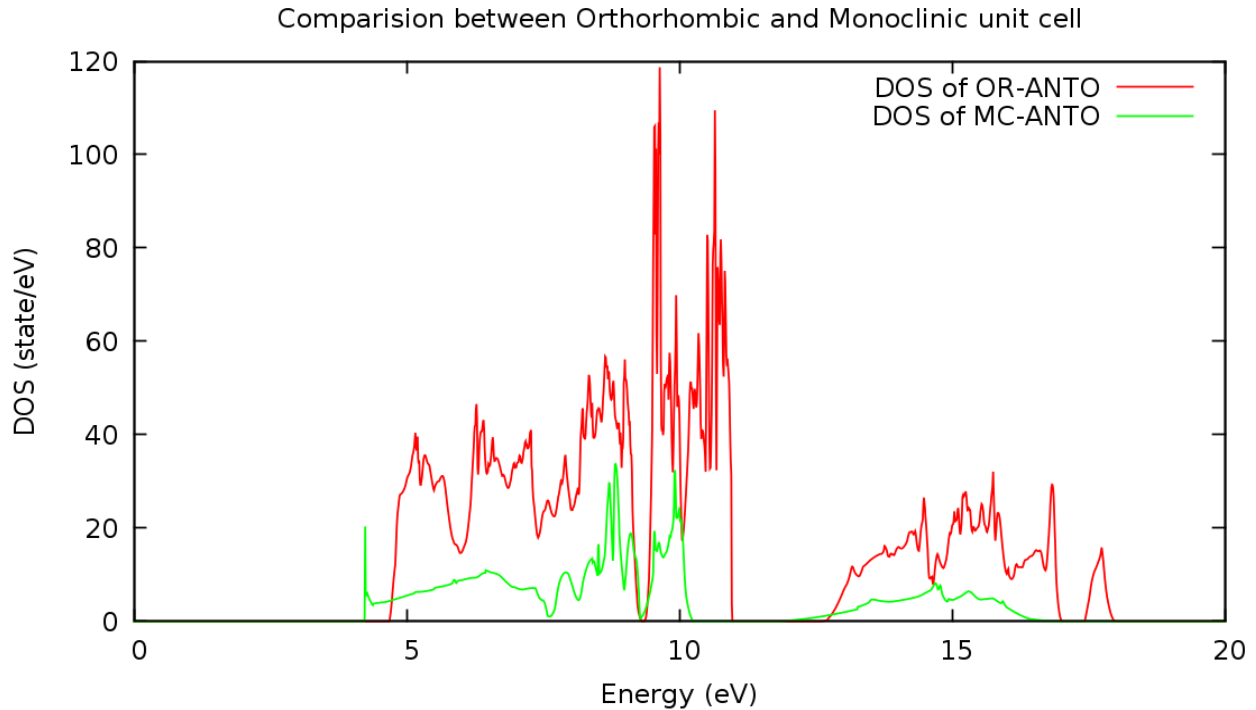


Fig. 3.4 Comparison between DOS of orthorhombic unit cell and monoclinic unit of ANTO

3.3. Projected Density of States

The plot of the total and projected density of electronic states (fig. 3.5) of ANTO for monoclinic structure, is calculated at the optimized structural parameters. As evident from plot (fig. 3.5), the valence band (VB) extends from 4 eV to 11.25 eV, and the states in the VB are primarily constituted of O-2p states. There is a weak hybridization between O-2p orbital and (a) Ta-5d and Nb-4d orbital at lower energy part of the VB, and (b) Ag-4d orbital in higher energy part of the VB. Such hybridization between cation and anion orbital results in mixed ionic-covalent bonding in ANTO. The states in the conduction band (CB) in the energy range ~12.0–17.0 eV arise primarily from the Ta-5d and Nb-4d orbital in addition to Ag-5s states with weaker contribution.

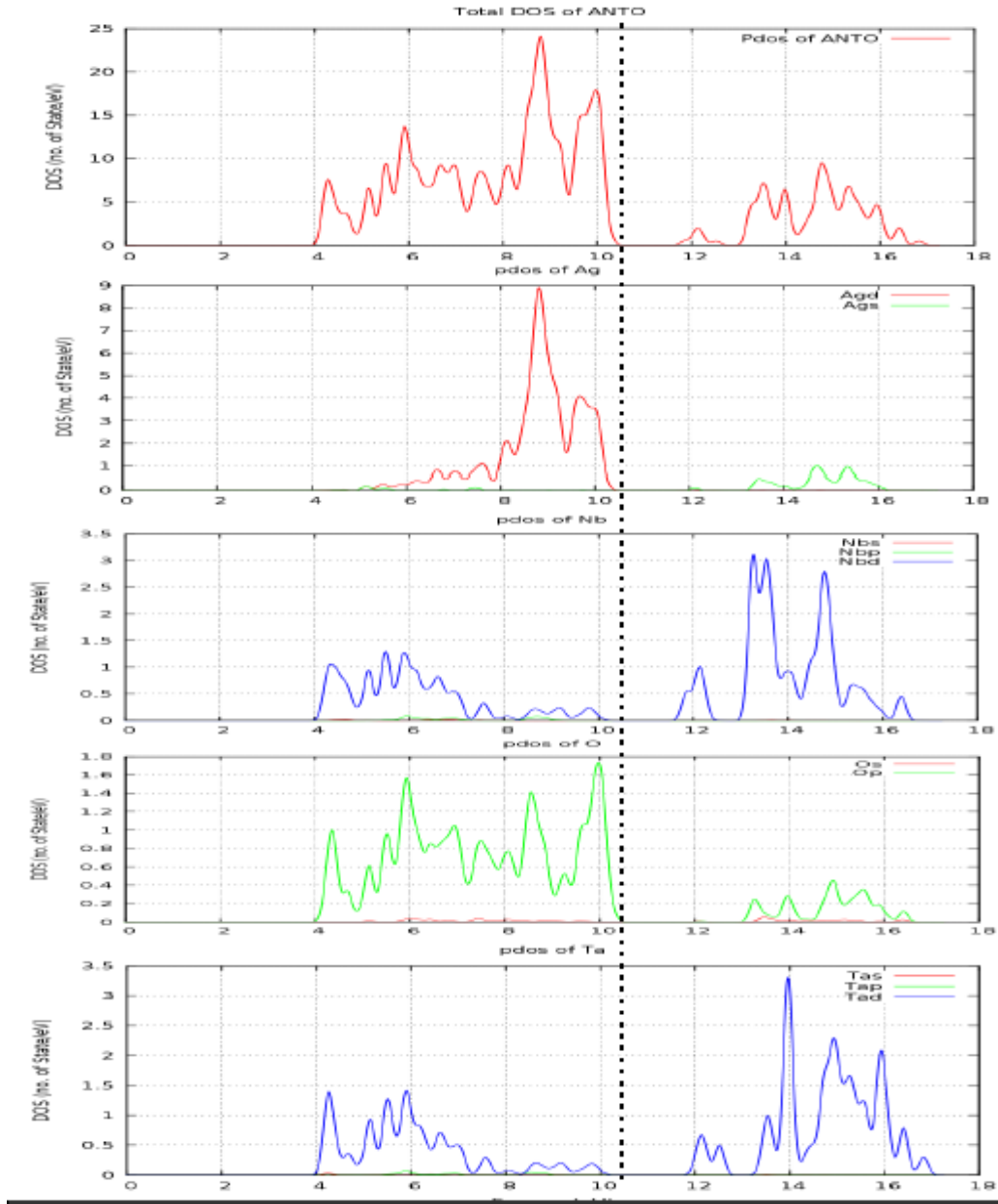


Fig. 3.5 Projected density of state of monoclinic unit cell of ANTO

Here, the plot (fig. 3.5) is of ANTO having monoclinic structure. First curve represents the Density of State of ANTO, second curve represents projected density of state of Ag (red curve is for Ag-4d and green curve is Ag-s), third curve is of Nb where blue curve represents most of the contribution is coming from Nb-d, Fourth curve represents O and O-p is contributing to the VB and CB and the last curve represents Ta which is similar to Nb curve and here also Ta-d contribution is more and mostly in the lower VB and in CB. Dotted line represents the uppermost valence band (Fermi level).

3.4. Band Structure

The Band Structure of a solid describes those ranges of energy that an electron within the solid may have which is called *energy bands* or *allowed bands* or simply *bands* and ranges of energy that it may not have called *band gaps* or *forbidden bands*. When multiple atoms join together to form a molecule, their atomic orbital's combine to form molecular orbital. As more atoms are brought together, the molecular orbital extend larger and larger, and the energy levels of the molecule will become increasingly dense [8][9].

The most important bands and band gaps—those relevant for electronics—are those with energies near the Fermi level. The bands near Fermi level are Conduction band and valence band respectively.

In an insulator or semiconductor, the Fermi level is surrounded by a band gap, referred to as *the band gap*. The closest band above the band gap is called *the conduction band*, and the closest band beneath the band gap is called *the valence band*. The name "valence band" was coined by analogy to chemistry, since in many semiconductors the valence band is built out of the valence orbital [9].

In band calculation, the path in reciprocal space [7], along which band calculation is done, is:

$$\Gamma\text{-X-M-}\Gamma\text{-Z-R-A-Z|X-R|M-A}$$

[7] for monoclinic structure (fig. 3.6).

$\times b_1$	$\times b_2$	$\times b_3$		$\times b_1$	$\times b_2$	$\times b_3$	
0	0	0	Γ	0	$\frac{1}{2}$	$\frac{1}{2}$	R
$\frac{1}{2}$	$\frac{1}{2}$	$\frac{1}{2}$	A	0	$\frac{1}{2}$	0	X
$\frac{1}{2}$	$\frac{1}{2}$	0	M	0	0	$\frac{1}{2}$	Z

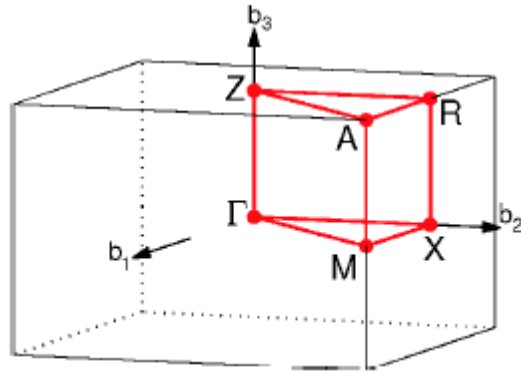


Fig. 3.6 monoclinic unit cell with symmetric k- points [7]

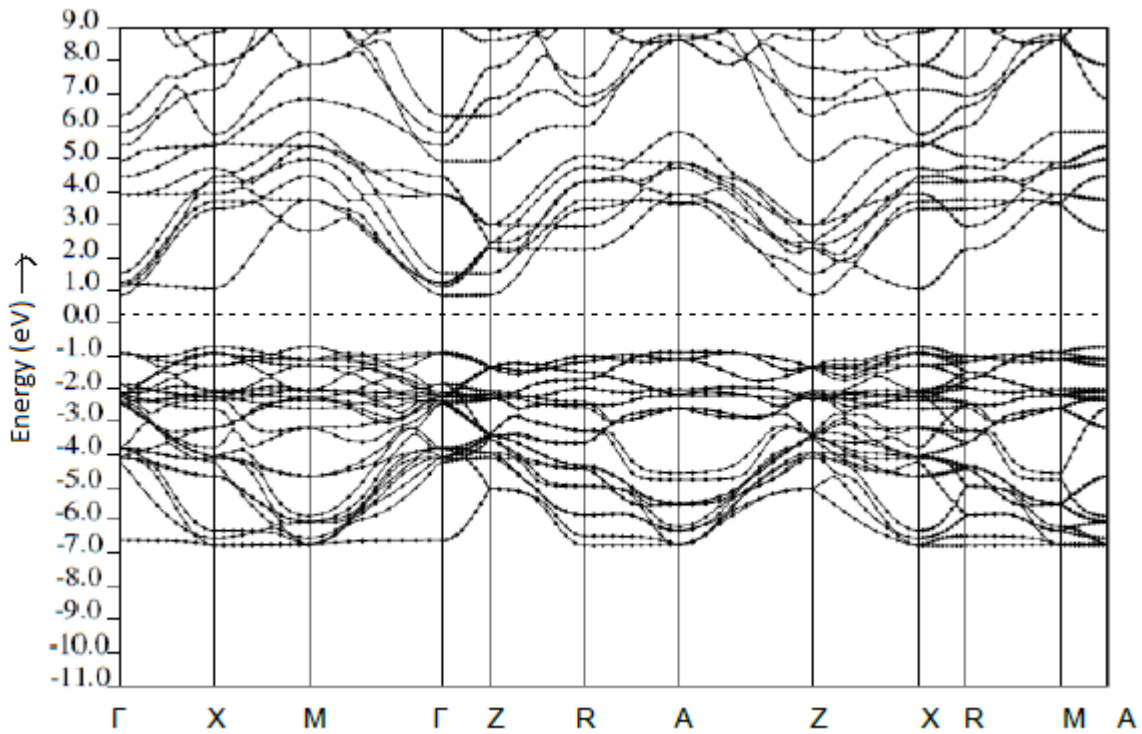


Fig. 3.7. Band Structure of ANTO here y- axis is represent the energy level (eV) and x-axis is the symmetry k-point

In the fig. 3.7, the origin is at the Fermi level =11.0336 eV. The band gap is ~ 3 eV and 2eV which lies in the semiconductor region but DFT underestimates the band gap. There are few direct band gaps in the compound. Band Structure of the compound is consistent with the DOS curve (fig. 3.8) and it has a direct band gap between the valence and conduction band at Γ - point. Also, upper level of valence band are filled so introducing p-type impurity can improve its conductivity. The lower level of conduction band is at the Γ -point and Z-point and 2nd lower level of conduction band is at M-point.

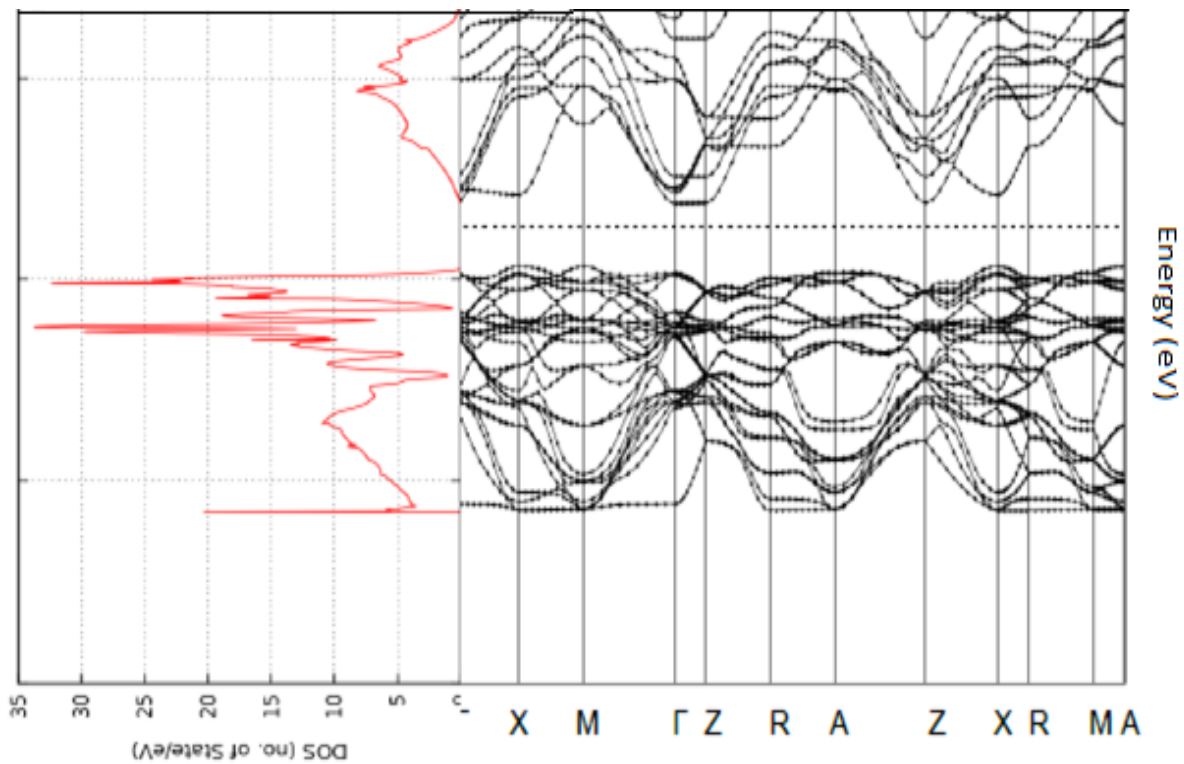


Fig. 3.8 Band structure of ANTO is consistent with the DOS curve with fermi level at 11.25 eV

3.5. Charge Density

Charge density is measure of electric charge per unit volume of space in one , two and three dimension. I have calculate the charge density in 2-dimension with the miller index (011). Plane with miller indices (011) can be viewed in fig. 3.9.

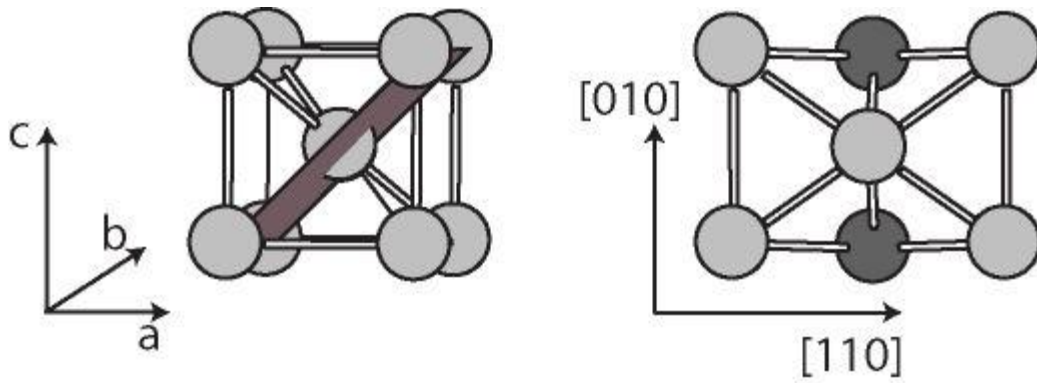


Fig. 3.9 (011) plane with their miller indices

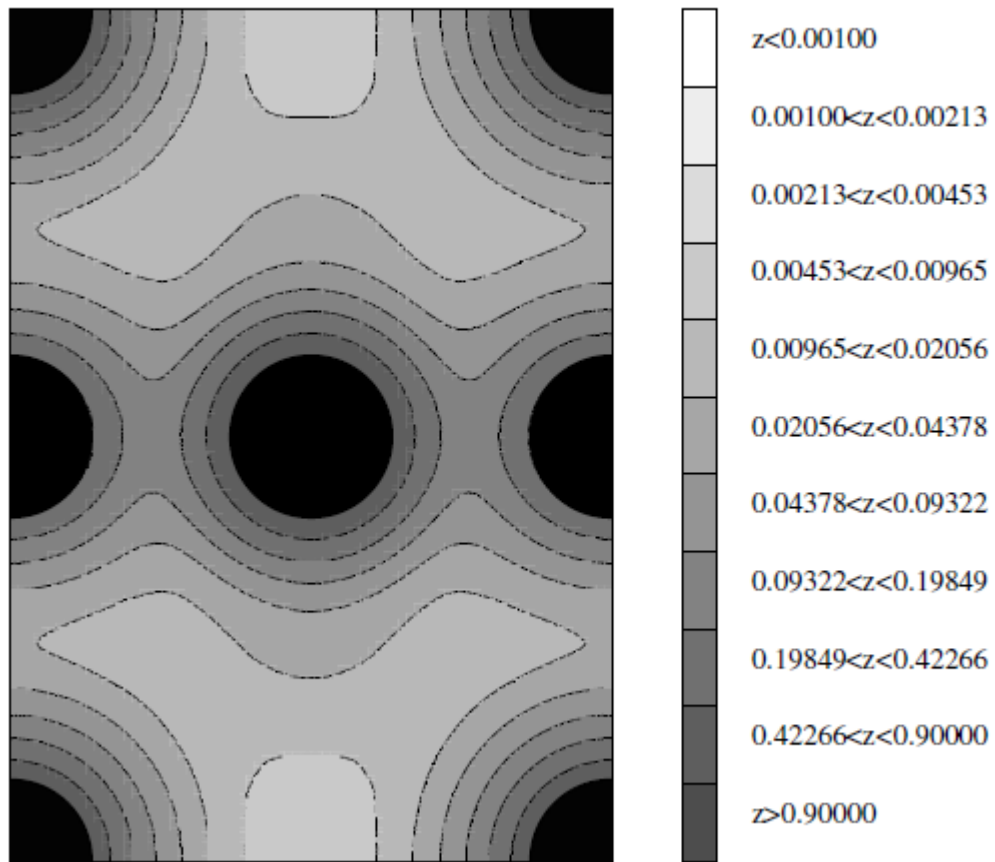


Fig. 3.10 Charge density plot for ANTO for Monoclinic Structure for (011) plane and z represents the charge density in the unit cell

In fig. 3.10, the Charge Density is plotted for ANTO compound for monoclinic structure. The plane surface with miller indices (011) is shown in the plot of the compound. The Corner atom of the unit cell is Silver, Body center is shared by Ta and Nb and Face atoms are Oxygen. Black portion of the plot represents the core of the atom. This plot shows that the electrons are accumulated almost spherically around Ag and therefore represents an ionic bond between O and Ag. The electron accumulation between the O and Ta or Nb atoms is aspherical in character indicate ionic- covalent interaction between the O and Ta or Nb atoms. Due to high electronegativity of O , bond between O and Ta (Nb) is ionic - covalent. There is almost no electronic charge between the two silver atoms.

3.5. Phonon

A phonon is a quantum mechanical description of a vibrational motion in which a lattice of atoms or molecules uniformly oscillates at single frequency. In classical mechanics this is known as a normal mode [8].

The phonon calculation is done at Γ -point in the brillouin zone because at Γ - point the frequency of the acoustic phonon converges to zero, regardless of polarization [15]. But optical phonons are phonons in which the atoms in the unit cell move out of phase in the long wavelength limit therefore at the gamma point, the frequency is not zero i.e. they have a finite energy. Also, there can be no more than 3 polarization of acoustic phonons (1 longitudinal and 2 transverse) for each wave vector and hence first three frequencies of the phonon calculation are zero and $3N-3$ non zero optical phonon frequencies in both type of unit cells of ANTO.

For monoclinic structure we have 30 modes in which first 3 are acoustic phonon modes and 27 non zero optical phonon modes and for orthorhombic structure we have 120 modes in which 117 modes are non zero which corresponds to optical branch. A negative frequency in phonon calculation represents that the compound is unstable. When the phonon frequencies are visualised (using xcrysdn or something else) it is seen that higher frequencies corresponds

to oxygen and lower frequencies corresponds to heavier atoms (Ag, Ta and Nb) implying frequency is inversely proportional to mass.

From the phonon frequency band (fig. 3.11) for both type of unit cells in GGA approximation, we get that the phonon frequency lies between 0 to 925 cm^{-1} for both type of unit cells. For monoclinic unit cell phonon plot is at top (fig. 3.11 (1)) and in the plot it can be seen that there is absolutely no frequency between ~ 125 to 225 cm^{-1} , ~ 350 to 550 cm^{-1} and ~ 600 to 830 cm^{-1} range and only one frequency between 250 cm^{-1} and 525 cm^{-1} . Phonon frequency is dense in the lower frequency region that is in between 50 to 125 cm^{-1} implying that heavy atoms are contributing more to the phonon calculation at Γ - point for monoclinic unit cell. For orthorhombic unit cell phonon plot is at the bottom (fig. 3.11 (2)) and there is no phonon frequency between 425 to 475 cm^{-1} and 650 to 725 cm^{-1} range. Here also, phonon frequency is dense in the region of 0 to 425 cm^{-1} implying heavy atoms are contributing more to the phonon frequency and in the range of 75 to 125 cm^{-1} frequencies are very close at Γ - point for orthorhombic unit cell.

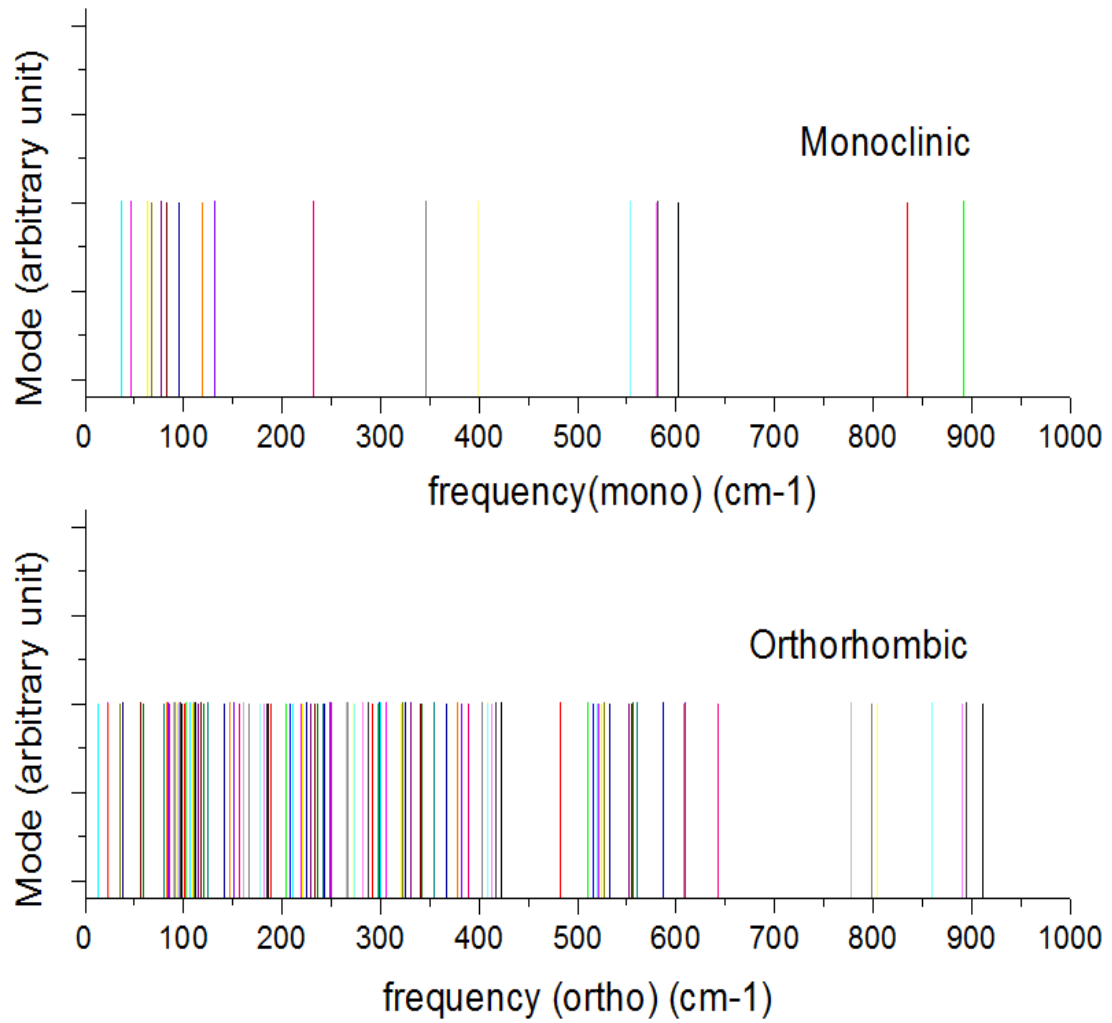


Fig. 3.11 Phonon Frequency band in (cm⁻¹). (1) plot at the top represent the frequency band for monoclinic unit cell and (2) plot at the bottom represents the frequency band for orthorhombic unit cell.

From fig.3.12, It can be seen that phonon frequency distribution for LDA and GGA approximation is almost same few value differences.

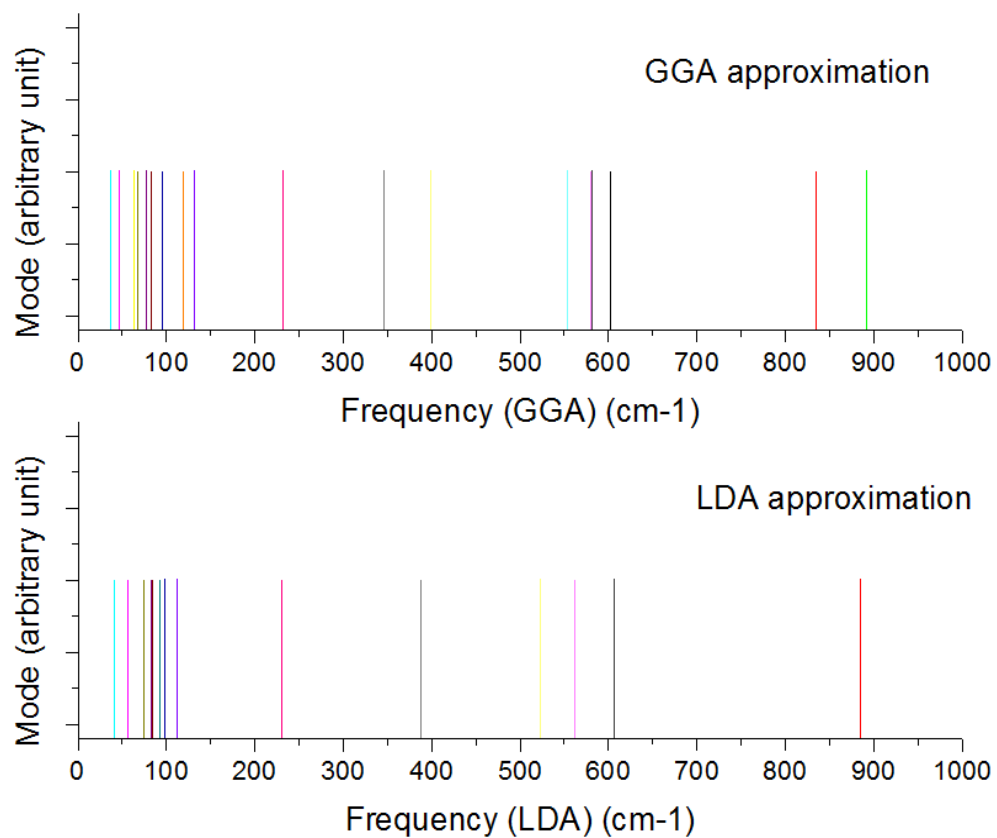


Fig. 3.12 Phonon Frequency band in (cm^{-1}). (1) plot at the top represent the frequency band for monoclinic unit cell with GGA approximation and (2) plot at the bottom represents the frequency band for monoclinic unit cell with LDA approximation.

Chapter 4.

4. Conclusion and Discussion

4.1. Conclusion

- The relaxed lattice parameter obtained using GGA approximation is more close to experimentally found lattice parameter. Percentage error in the volume of monoclinic cell is 2.5% for LDA and 0.6% for GGA which is less than 5% so relaxed structure is acceptable and for orthorhombic cell it is ~5% for GGA potential. Since, percentage error is less in GGA potential so calculation is pursued for GGA potential.
- DOS curve for Monoclinic and orthorhombic Structure suggests that the compound is insulator or semiconductor with upper-most valence band at ~11.25 eV and ~11.75eV respectively. From PDOS curve, there is a weak hybridization between O-2p orbital and (a) Ta-5d and Nb-4d orbital at lower energy part of the VB, and (b) Ag-4d orbital in higher energy part of the VB. Such hybridization between cation and anion orbital results in mixed ionic-covalent bonding in ANTO. The states in the conduction band (CB) arise primarily from the Ta-5d and Nb-4d orbital in addition to Ag-5s states with weaker contribution.
- DFT underestimates the band gap but there are few direct band gaps in the compound. Band Structure of the compound is consistent with the DOS curve and it has a direct band gap between the valence and conduction band at Γ - point. Also, upper level of valence band are filled so introducing p-type impurity can improve its conductivity.
- Charge density of this compound gives that the compound has ionic property. The electrons are accumulated almost spherically around Ag and therefore represents an ionic bond between O and Ag. The electron accumulation between the O and Ta or Nb atoms is aspherical in character indicate ionic- covalent interaction between the O and Ta or Nb atoms. Due to high electronegativity of O , bond between O and Ta (Nb) is ionic - covalent. There is almost no electronic charge between the two silver atom.
- For monoclinic structure we have 30 modes in which first 3 are acoustic phonon modes

and 27 non zero optical phonon modes and for orthorhombic structure we have 120 modes in which 117 modes are non zero which corresponds to optical branch. A negative frequency in phonon calculation represents that the compound is unstable. The higher phonon frequencies corresponds to oxygen and lower frequencies corresponds to heavier atoms (Ag, Ta and Nb) implying frequency is inversely proportional to mass. Phonon frequency is dense in the lower frequency region that is in between 0 to 400 cm^{-1} which corresponds to Ag-O and Nb-O/Ta-O implying that heavy atoms are contributing more to the phonon calculation in the lower frequency range and O atom is contributing to the higher frequency range at Γ - point.

4.2. Discussion

I have used DFT to do the ab-initio analysis of the ANTO compound's structural and electronic properties. DFT uses LDA and GGA to find the potential but in LDA the compounds relaxed volume error is higher than the GGA because GGA provides potential as functional of density and its gradient. For DOS calculation scf and nscf calculation is done. In nscf calculation the fermi level and occupation numbers are calculated which is used in calculating DOS of a compound.

Also, DFT does not predicts the band gap correctly . To find the band gap theoretically other methods can be used. DFT uses plane wave self consistent field which is generated with the exact Kohn-Sham potential $v_{\text{eff}}(r)$, and even this underestimates band gap but gives perfect band structure that is perfect valence and conduction band.

Phonon calculation is two step process. First, step is to find the ground state atomic and electronic configuration and second step is calculate the phonon using Density functional perturbation theory. Phonon calculation is done at gamma point where, acoustic modes are zero but optical modes are non zero. Phonons frequency is inversely proportional to the mass of atoms in the compound.

Chapter 5.

5. Reference

- [1] N. Izyumskayaa; Ya. Alivova; H. Morkoça , Oxides, Oxides, and More Oxides: High- κ Oxides, Ferroelectrics, Ferromagnetics, and Multiferroics, Solid state and material science , Dec. 2009
- [2] Matjaz Valant and Danilo Suvorov, New High-Permittivity $\text{AgNb}_{1-x}\text{Ta}_x\text{O}_3$ Microwave Ceramics: Part I, Crystal Structures and Phase-Decomposition Relations *J. Am. Ceram. Soc.*, **82**, 81–87 (1999)
- [3] Igor Levin,¹ Victor Krayzman,¹ Joseph C. Woicik, Structural changes underlying the diffuse dielectric response in AgNbO_3 , *PHYSICAL REVIEW B* **79**, 104113 _2009
- [4] I. Levin,^{*,†} J. C. Woicik,[†] A. Llobet, Displacive Ordering Transitions in Perovskite-Like $\text{AgNb}_{1/2}\text{Ta}_{1/2}\text{O}_3$, *Chem. Mater.* 2010, 22, 4987–4995 4987
DOI:10.1021/cm101263p
- [5] Manish K. Niranjana, Saket Asthana, First Principles study of lead free piezoelectric AgNbO_3 and $(\text{Ag}_{1-x}\text{K}_x)\text{NbO}_3$ solid solutions, *Solid State Communications* 152 (2012) 1707–1710
- [6] Manish K. Niranjana, T. Karthik, Saket Asthana, Jaysree Pan, and Umesh V. Waghmare, Theoretical and experimental investigation of Raman modes, ferroelectric and dielectric properties of relaxor $\text{Na}_{0.5}\text{Bi}_{0.5}\text{TiO}_3$, <http://dx.doi.org/10.1063/1.4804940>
- [7] Wahyu Setyawan and Stefano Curtarolo, High-throughput electronic band structure calculations: challenges and tools, arXiv:1004.2974v1 [cond-mat.mtrl-sci] 17 Apr 2010
- [8] Charles Kittel, *Introduction to Solid State Physics*, 8th Edition, Chapter 4
- [9] P.Y. Yu, M. Cardona, *Fundamentals of Semiconductors*, Graduate Texts in Physics, 4th ed.,
- [10] H. Eschrig, *The Fundamentals of Density Functional Theory*, Chapter 2
- [11] H. Eschrig, *The Fundamentals of Density Functional Theory*, Chapter 4
- [12] H. Eschrig, *The Fundamentals of Density Functional Theory*, Chapter 6
- [13] H. Eschrig, *The Fundamentals of Density Functional Theory*, Chapter 7

- [14] Kohn, W.; Sham, L. J. (1965). "Self-consistent equations including exchange and correlation effects". *Physical Review* **140** (4A): A1133–A1138
- [15] Perdew, John P; Chevary, J A; Vosko, S H; Jackson, Koblar, A, (1992). "Atoms, molecules, solids, and surfaces: Applications of the generalized gradient approximation for exchange and correlation". *Physical Review B* **46** (11): 6671
- [16] Becke, Axel D (1988). "Density-functional exchange-energy approximation with correct asymptotic behavior". *Physical Review A* **38** (6): 3098
- [17] Density-Functional Theory of Atoms and Molecules, R.G Parr and W. Yang, Oxford University Press, New York (1989).
- [18] Peter Y Yu, Manuel Cardona, Fundamentals of Semiconductors
- [19] I. N. Belayaev, T. G. Lupeiko, and V. B. Nalbandyan, "Rhombohedral Metatantalates of Silver and Solid Solutions from the (Ag,Na)TaO₃ and Ag(Nb,Ta)O₃ Systems," *Kristallografiya*, **23** [3] 620–21 (1978).
- [20] M. Pawelczyk, "Phase Transitions in AgTa_xNb_{1-x}O₃ Solid Solutions," *Phase Transitions*, **8**, 273–92 (1987).
- [21] Bachelet, G. B.; Hamann, D. R.; Schlüter, M. (October 1982), "Pseudopotentials that work: From H to Pu", *Physical Review B* (American Physical Society) **26** (8): 4199–4228.
- [22] Vanderbilt, David (April 1990), "Soft self-consistent pseudopotentials in a generalized eigenvalue formalism", *Physical Review B* (American Physical Society) **41** (11): 7892–7895.

Thank You !!